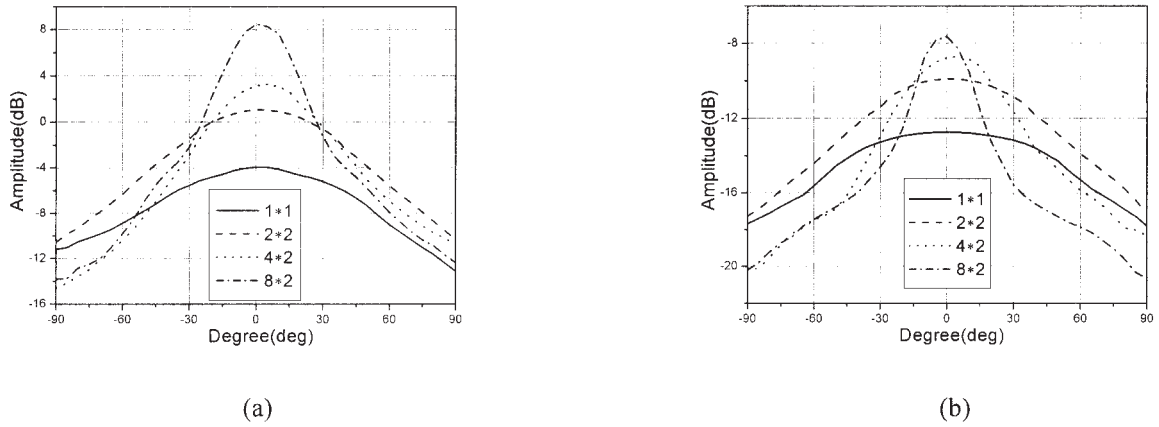

Figure 5 Pattern in the H-plane for receiving: (a) energy pattern; (b) peak amplitude pattern

Figure 3 shows the peak value of the received pattern array (E_p) is proportional to the square root of the array elements number (N) in the boresight, that is,

$$E_p \propto \sqrt{N}. \tag{3}$$

This shows that the total field of the array is determined by the vector summation of the fields radiated by the individual elements and the coupling between antennas has little effect on the pattern, because the UWB antenna has local-region effects, that is, the coupling only takes effect where the pulse wave travels.

The pattern with different amounts of space between the elements but the same number of elements is shown in Figure 4, which shows that the pattern is about identical, and the array with larger separation of the elements has narrower beam width for larger distance, and longer time delay in the off-axial direction. When the elements' space d is larger than $c\tau$, that is, $d > c\tau$, there will be a noninterfering region [7] (τ is the pulse width and c is the speed of wave propagation). Thus, the beam pattern is narrower with larger separation of the elements. In the figure, when the space between elements is larger than 1.0 m, there is a noninterfering region. There will not be a "grating lobe" as that of the narrowband antenna array; however, a "side lobe" will appear because the short pulse from the elements of the UWB array interfere constructively in the off-axial directions (in addition to the axial direction) and interfere destructively in the remaining space. The figure also shows the maximum value of patterns is a little larger as the elements' space is larger.

Figure 5 is the energy pattern and peak amplitude pattern with relative 25-cm displacement between the elements, which shows that the more elements there are along a line in the H-plane, the narrower the pattern beam in the H-plane. Though the relative distance between the elements is the same, the maximum time delay increases as the elements increase. The array beam varies more sharply.

6. CONCLUSION

The TSA suits the receiving antenna array due to its light weight and planar structure. The array can reduce the beamwidth and increase the receiving gain as compared to the single antenna, which can be used in practical radar systems.

REFERENCES

1. K.L. Shlager, G.S. Smith, and J.G. Maloney, Optimization of bow-tie antennas for pulse radiation, IEEE Trans Antennas Propagat 42 (1994), 975–982.
2. K.L. Walton and V.C. Sundberg, Broadband ridged horn design, Microwave J 1964, 96–101.
3. K.S. Yngvesson, D.H. Schaubert, and T.L. Korzeniowski, Endfire tapered slot antennas on dielectric substrates, IEEE Trans Antennas Propagat 33 (1985), 1392–1400.
4. R.T. Lee and G.S. Smith, A design study for the basic TEM horn antenna, IEEE Antennas Propagat Mag 46 (2004), 86–92.
5. B. Schiek and J. Köhler, An improved microstrip to microslot transition, IEEE Trans Microwave Theory Tech 24 (1976), 231–233.
6. W.J. Welch, Reciprocity theorems for electromagnetic fields whose time dependence is arbitrary, IRE Trans Antennas Propagat 8 (1960), 68–73.
7. J.L. Schwartz and B.D. Steinberg, Ultrasparse ultrawideband arrays, IEEE Trans Electromagn Compat 45 (1998), 376–393.
8. O.E. Allen, D.A. Hill, and A.R. Ondrejka, Time-domain antenna characterizations, IEEE Trans Electromagn Compat 35 (1993), 339–345.
9. A. Shlivinski, E. Heyman, and R. Kastner, Antenna characterization in the time domain, IEEE Trans Antennas Propagat 45 (1997), 1140–1149.

INVESTIGATING THE PERFORMANCE OF MIMO SYSTEMS FROM AN ELECTROMAGNETIC PERSPECTIVE

Marek E. Bialkowski,[1] Peerapong Uthansakul,[1] Konstanty Bialkowski,[1] and Salman Durrani[2]
[1] School of Information Technology & Electrical Engineering
The University of Queensland
Brisbane, QLD 4072, Australia
[2] Department of Engineering
The Australian National University
Canberra, ACT 0200, Australia

Received 2 January 2006

ABSTRACT: *Multiple input multiple output (MIMO) wireless systems use multiple element antennas (MEAs) at the transmitter (TX) and the receiver (RX) in order to offer improved information rates (capacity) over conventional single antenna systems in rich scattering environments. In this paper, an example of a simple MIMO system is considered in which both antennas and scattering objects are formed by wire dipoles. Such a system can be analyzed in the strict electromagnetic (EM) sense and its capacity can be determined for varying array size, interelement spacing, and distributions of scatterers. The EM model of this MIMO system can be used to assess the validity of single- or double-bounce scattering models for mixed line of sight (LOS) and*

non-line of sight (NLOS) signal-propagation conditions. © 2006 Wiley Periodicals, Inc. Microwave Opt Technol Lett 48: 1233–1238, 2006; Published online in Wiley InterScience (www.interscience.wiley.com). DOI 10.1002/mop.21664

Key words: *multiple-input-multiple-output (MIMO); array antennas; mutual coupling; channel capacity and propagation modelling*

1. INTRODUCTION

In the last decade, wireless cellular communications has experienced rapid growth in the demand for provision of new wireless multimedia services such as Internet access, multimedia data transfer, and video conferencing. In order to meet this demand and to overcome the limited capacity of conventional single input single output (SISO) systems, the use of multiple element antennas (MEAs) has been proposed [1]. When MEAs are employed to create multiple inputs and outputs at the transmitter (TX) and receiver (RX) sides, such systems are named MIMO systems [2–7].

Initial work concerning prediction of the performance of MIMO systems has been done by researchers working mostly in the field of information theory [2–7]. It has been shown that MIMO systems offer increased capacity over SISO counterparts when the fading is independent in the links between different pairs of TX and RX antennas [5]. The usual assumption, leading to increased information rate, is that the channel matrix is formed by independent identically distributed (i.i.d.) complex Gaussian elements with unit variance [2]. However, how such a communications channel (as given by the physical scatterers) arises or can be realized in practice has not been stated. Practical issues which are of concern to MIMO system designers include the TX and RX array geometry and orientation, the number of antenna elements, and interelement spacing. The array spacing is an especially important parameter, as it is related to the compactness of MIMO systems. However, small array spacing affects both power transmission and reception due to mutual coupling between antenna elements. Also, it affects the statistical properties of received signals.

Recently, the effect of mutual coupling due to varying array spacing on MIMO capacity has been reported in [8–11]. Computer simulations and measurements have been used for this purpose. In [8], by using the so-called single-bounce scattering (SBS) model, it was demonstrated that mutual coupling may reduce the correlation between antenna signals, thus increasing the capacity. This conclusion has been supported by the measurements in [12] and the theoretical results obtained in [10] using the network-theory analysis framework.

It has to be noted that scattering models used to arrive at the above conclusions are often simplified. For example, in the studies presented in [8, 10], the condition of non-line of sight (NLOS) signal propagation has been used. Such an assumption may be invalid for many indoor/outdoor scenarios because of presence of the LOS signal component. The other issue not investigated is the TX/RX antennas orientation.

In order to provide suitable answers to the abovementioned issues and questions, an analyzing of MIMO system from a strict electromagnetic (EM) perspective is necessary [13]. This paper addresses this problem by analyzing in an accurate manner the performance of a simple MIMO system, in which TX/RX array antennas as well as scatterers are formed by half-wavelength dipoles.

2. ELECTROMAGNETIC MODEL OF A MIMO SYSTEM COMPOSED OF WIRE ANTENNAS

The simple MIMO system considered is defined as follows:

1. Both the TX and RX arrays, separated by distance D, are formed by half-wavelength parallel wire dipoles, arranged in an arbitrary configuration and oriented in a horizontal plane (only the 2D distribution case is considered here). The number of antennas in the TX and RX arrays is denoted respectively by N_T and N_R.
2. N_S scatterers surrounding the TX and RX are also formed by half-wavelength parallel wire dipoles, arranged in arbitrary configuration and distribution in the same plane as the TX and RX antennas.
3. The scatterers surrounding the TX and RX sites form a static or random assembly. The random assembly is formed by many different static cases, in which the locations of scattering objects are generated by a random process.

Assuming that the TX and RX arrays are arranged as linear arrays with interelement spacings d_T and d_R, respectively, the system model, here called the EM model, is illustrated in Figure 1. The objective is to determine, at a given frequency, the complex channel matrix **H** and then the channel capacity C.

2.1. MIMO Channel Characterization Using Impedance Matrix

The interactions between the entire set of antennas and scatterers are initially described by the impedance matrix **Z.** For dipoles, the mutual impedance can easily be calculated using the classical induced electromagnetic force (EMF) method [14, 15]. For the side-by-side configuration, the value of the mutual impedance Z_{mn} between the m^{th} and n^{th} dipoles is given by [14]:

$$Z_{mn} = \begin{cases} 30[0.5772 + \ln(2\beta l) - C_i(2\beta l)] \\ \quad + j[30S_i(2\beta l)], & m = n \\ 30[2C_i(u_0) - C_i(u_1) - C_i(u_2)] \\ \quad - j[30(2S_i(u_0) - S_i(u_1) - S_i(u_2)), & m \neq n \end{cases}, \quad (1)$$

where $\beta = 2\pi/\lambda$ is the wave number, $l = \lambda/2$ is the dipole length, and the constants are given by [16]:

$$u_0 = \beta d_h,$$

$$u_1 = \beta(\sqrt{d_h^2 + l^2} + l),$$

$$u_2 = \beta(\sqrt{d_h^2 + l^2} - l), \quad (2)$$

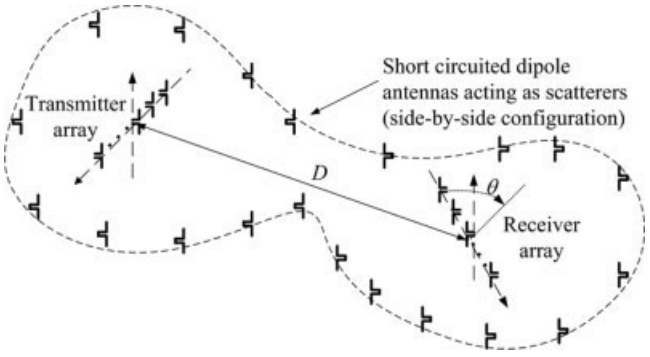

Figure 1 General configuration of the MIMO system used in an electromagnetic model

where d_h is the horizontal distance between the two dipole antennas and $C_i(u)$ and $S_i(u)$ are the cosine and sine integrals, respectively, defined as [15]:

$$C_i(u) = \int_{\infty}^{u} \frac{\cos(x)}{x}\, dx,$$

$$S_i(u) = \int_{0}^{u} \frac{\sin(x)}{x}\, dx. \tag{3}$$

It has to be noted that while calculating Z_{mn}, we assume that the n^{th} dipole is excited with current, while all the remaining dipoles are open-circuited. Calculations of Z_{mn} require considering the presence of only two dipoles: the m^{th} and n^{th}. The reason for this is that all the remaining open-circuited half-wavelength dipoles do not resonate and are transparent to the incident waves.

2.2. Calculation of the Channel Matrix

Once **Z** is calculated, the next step is to determine the channel matrix **H.** For this purpose, we assume that dipoles of the TX array are excited one by one. For each case, we calculate the voltage ratios between the excited dipole in the TX antenna and every dipole in the RX antenna TX, that is, we find the ratio $h_{pq} = V_p/V_q$, where the subscript q indicates the excited dipole in the TX antenna and the subscript p indicates the dipole in the RX antenna. In this case, the unexcited dipoles in the TX and RX antennas are assumed to be match terminated, assuming $Z_L = Z_A^*$, where $Z_A = 73 + j42.5$ (in Ohms) is the input impedance of the half-wavelength dipole in isolation and * denotes complex-conjugate operation. The scatterers are assumed to be short circuited dipoles. Other load conditions can also be included but are not considered here.

Having specified the load conditions, we can solve for the currents on the dipoles using the general relationship

$$\mathbf{I} = (\mathbf{Z}_{LOAD})^{-1}\mathbf{V}, \tag{4}$$

where $\mathbf{Z}_{LOAD}$ is the modified mutual-impedance matrix under load conditions. The currents in the RX antenna dipoles are converted into voltages using

$$V_p = -Z_L I_p. \tag{5}$$

Assuming the excitation voltage is 1, the values of V_p directly give the entries of the channel matrix **H.**

2.3. MIMO Channel Capacity

The MIMO capacity can be calculated using two alternative conditions [16] of a fixed received power or a fixed transmitted power. The most frequently used is the one involving the fixed received power, or fixed signal-to-noise Ratio (SNR), given by [2]:

$$C_{P_R=const} = \log_2 \det\left[\mathbf{I} + \frac{\rho}{N_T}\mathbf{H}\mathbf{H}^{\dagger}\right], \tag{6a}$$

where $C_{P_R=const}$ is the instantaneous channel capacity corresponding to a given realization of channel matrix **H,** $\rho = P_T/P_N$ with P_T the total transmitted power and P_N the noise power at each receiving antenna, **I** is an $N_R \times N_R$ identity matrix, and † denotes Hermitian or complex-conjugate and transpose matrix operation. The assumption of fixed SNR or ρ requires suitable normalization **H** to make comparisons with the i.i.d. channel. Here, the channel matrix is normalized such that $\|\mathbf{H}\|_F^2 = N_T N_R$ for i.i.d. channel, where $\|(\cdot)\|_F$ denotes the Frobenius norm [8].

For the case of fixed transmitted power, the MIMO capacity is calculated using Eq. (6b) as follows:

$$C_{P_T=const} = \log_2 \det\left[\mathbf{I} + \frac{P_T}{N_T P_N}\mathbf{H}\mathbf{H}^{\dagger}\right]. \tag{6b}$$

In this case, no normalization is used for **H** so that the total received power P_T and thus ρ can vary. However, as observed in Eq. (6b), the calculations of $C_{P_T=const}$ require fixing the value of noise power P_N.

Note that expressions Eqs. (6a) and (6b) assume a so-called independent transmission scheme in which the transmitted signals are uncorrelated and of equal power.

3. TWO-RING DOUBLE BOUNCE SCATTERING MODEL

In order to perform comparisons with approximate models, a two-ring double-bounce scattering (DBS) model is chosen, as shown in Figure 2. In contrast to [8, 10], we assume the presence of both LOS and NLOS signal-propagation conditions. Similarly, as in the EM model, TX and RX antennas are formed by linear parallel wire dipoles and the distance between them is fixed and given by D. Interactions and thus the effect of mutual coupling between individual antenna elements within the TX and RX arrays are initially described by the impedance matrices, similarly as in the EM model. The obtained impedance matrices are converted into coupling matrices ($\mathbf{C}_T$ for transmitter and $\mathbf{C}_R$ for receiver, respectively) using standard conversion procedures [8, 17].

The elements of the channel matrix h_{rt} (denoting the transfer functions between t^{th} transmitting element and r^{th} receiving element) are obtained as [18]:

$$h_{rt} = \sqrt{\frac{1}{1+K}}\, h_{rt}^{NLOS} + \sqrt{\frac{K}{1+K}}\, h_{rt}^{LOS}, \tag{7}$$

where K is the Rician factor, which is defined as the power ratio between LOS and NLOS components. The LOS and NLOS components are given by

$$h_{rt}^{NLOS} = \sqrt{\frac{1}{S_R S_T}} \sum_{m=1}^{S_T} \sum_{n=1}^{S_R} \alpha_{mn} \exp\left(-j\frac{2\pi}{\lambda}(d_{mt} + d_{nm} + d_{rn})\right),$$

$$h_{rt}^{LOS} = \exp\left(-j\frac{2\pi}{\lambda} d_{rt}\right), \tag{8}$$

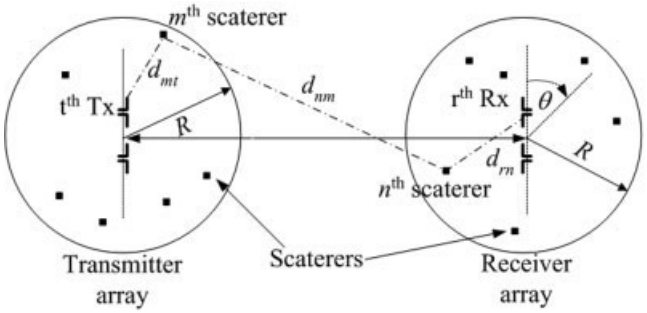

Figure 2 Configuration of the MIMO system used in a two-ring double-bounce scattering model

where α_{mn} is the scattering coefficient for the path of the m^{th} and n^{th} scatterers and is assumed as a normal complex random variable with zero mean and unit variance, d_{rn} is the distance between the r^{th} receiving element and the n^{th} scatterer, d_{nm} is the distance between the m^{th} and n^{th} scatterers, d_{mt} is the distance between the m^{th} scatterer and the t^{th} transmitting element, and d_{rt} is the distance between t^{th} transmitting element and r^{th} receiving element, as shown in Figure 2. S_T and S_R define the number of scatterers at TX and RX, respectively.

After determining $\mathbf{C}_{\mathrm{T}}$, $\mathbf{C}_{\mathrm{R}}$, and **H,** the MIMO system capacity is calculated from the following formula:

$$C = \log_2 \det\left(\mathbf{I} + \frac{\rho}{N_T}(\mathbf{C}_R\mathbf{H}\mathbf{C}_T)(\mathbf{C}_R\mathbf{H}\mathbf{C}_T)^{\dagger}\right). \tag{9}$$

For the case of fixed received power ($C_{P_R=const}$), the new channel matrix $\mathbf{H}'$ given by $\mathbf{H}' = \mathbf{C}_R\mathbf{H}\mathbf{C}_T$ is normalized such that $\|\mathbf{H}'\|_F^2 = N_T N_R$. For the case of fixed transmitted power, $C_{P_T=const}$, no such normalization is used.

Because the entries of **H** represent random processes, statistical values such as mean or variance are necessary to assess the MIMO capacity. Here, for all statistic cases, the average capacity is determined by using the mean value of C over random realizations of the channel matrix **H.**

4. RESULTS

The MIMO model involving wire dipoles as antennas and scattering objects is used in two case studies which concern static and random distributions of scattering objects. Comparisons with the DBS model are performed only for the case of random distribution of scattering objects.

4.1. Static Two-Ring EM Model of MIMO System

Without loss of generality, it is assumed that the number of TX and RX dipole arrays are $N_T = N_R = N$ with spacing given by d_T and d_R. $S_T = S_R = S$ scatterers are located over the perimeters of two circular rings of radius $R_T = R_R = R$. By proper selection of R, S, and D, various indoor and outdoor scenarios can be simulated.

4.1.1. Effect of Mutual Coupling

Figure 3 shows the plot of the capacity C (bps/Hz) versus RX array interelement spacing d_R (λ) for a 2×2 MIMO system, assuming $d_T = 1.0\lambda$, $R = 16\lambda$, $D = 50\lambda$, $\rho = 20$ dB, and $S = 100$ without and with interelement coupling included in the model. Calculations are performed under the condition of fixed received power and fixed transmitted power. In the latter case, the value of transmitted and noise power is selected such that ρ of 20 dB occurs for the array spacing $d_R = 1.0\lambda$. This choice is motivated by the fact that, for this spacing, mutual coupling is negligible. The results without mutual coupling are calculated by neglecting nondiagonal entries in the **Z** matrix for the TX and RX arrays.

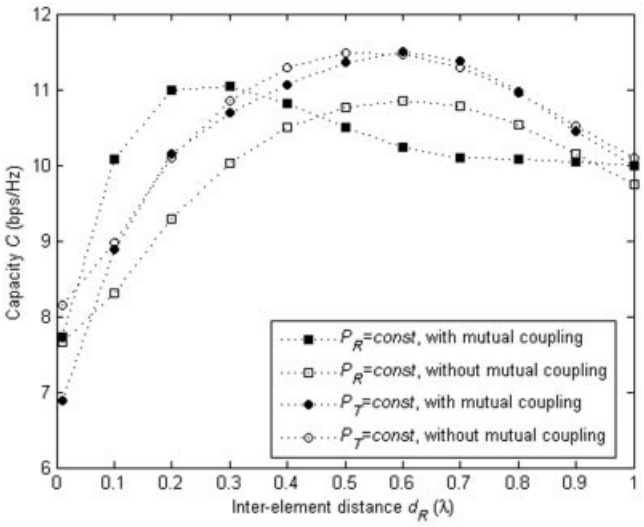

Figure 3 Capacity C (bps/Hz) vs. RX array interelement spacing $d_R(\lambda)$ for $N = 2$, $d_T = 1.0\lambda$, $R = 16\lambda$, $D = 50\lambda$, and $\rho = 20$ dB

It can be seen in Figure 3 that when the coupling is neglected capacity $C_{P_R=const}$ is nearly constant for $0.4\lambda < d_R < 1\lambda$, with a small ripple. However, for $d_R < 0.4\lambda$, there is a drop in capacity. For $d_R < 0.4\lambda$, the capacity $C_{P_R=const}$ (ignoring mutual coupling) is lower than that when mutual coupling is included. This drop can be attributed to the decreased correlation between the antenna elements for $d_R < 0.4\lambda$, as explained and demonstrated for the case of the 2×2 MIMO system in [5]. Quite different results are observed for capacity $C_{P_T=const}$ calculated under the condition of constant transmitted power. $C_{P_r-const}$ is nearly the same for $d_R > 0.1\lambda$, irrespective whether mutual coupling is included or neglected in calculations. The differences occur only in the region $d_R < 0.1\lambda$, where $C_{P_T=const}$ calculated under the mutual-coupling condition shows a significant drop. This is because mutual coupling is responsible for the impedance mismatch causing the drop in the received power and thus the capacity. When comparing $C_{P_T=const}$ and $C_{P_R=const}$ in Figure 3, it is clear that $C_{P_R=const}$ is smaller than $C_{P_T=const}$ for the array spacing $d_R > 0.4\lambda$. For $d_R < 0.4\lambda$, $C_{P_R=const}$ (with mutual coupling included in calculations) is greater than $C_{P_T=const}$. In the region $d_R > 0.4\lambda$, $C_{P_T=const}$ is greater than $C_{P_R=const}$ (neglecting mutual coupling). This confirms the findings observed in [8–11, 19], that is, in the small spacing region of $0.1\lambda < d_R > 0.4\lambda$, mutual coupling is beneficial in terms of increasing capacity irrespective of the assumption of constant received power or constant transmitted power.

4.1.2. Effect of Array Orientation

We consider the effect of the RX arrays' orientation on the capacity for 2×2 and 4×4 MIMO systems. Two cases, with and without mutual coupling, are considered in the EM model and the results are shown in Figure 4. Capacity $C_{P_R=const}$ is presented as a function of the angle of RX array rotation θ for $d_T = d_R = 1.0\lambda$, $R = 16\lambda$, $S = 100$, $D = 50\lambda$, and $\rho = 20$ dB. The RX array rotation angle θ is defined in both Figures 1 and 2. It can be seen that the broadside orientation ($\theta = 0°$) provides the best capacity while the end-fire ($\theta = 90°$) configuration provides the lowest capacity. The obtained results illustrate the same trend for both 2×2 and 4×4 MIMO systems, except that the capacity of the 4×4 MIMO is higher.

4.2. EM and DBS Statistical Models Comparison

Here, we compare the results for capacity obtained with the use of EM and DBS models. The investigated configuration is an area with two circular disks. As opposed to the static case discussed above, the scattering objects are randomly distributed within two circular rings instead of being located along the rings' perimeters. Uniform distributions of scatterers within the two-disk area are assumed. The results are obtained by averaging more than 500 channel realizations (random locations of scatterers).

4.2.1. Capacity Comparison Between EM and DBS Models

Figure 5 shows the plot of the capacity C (bps/Hz) versus RX array interelement spacing $d_R(\lambda)$ for a 2×2 MIMO system assuming

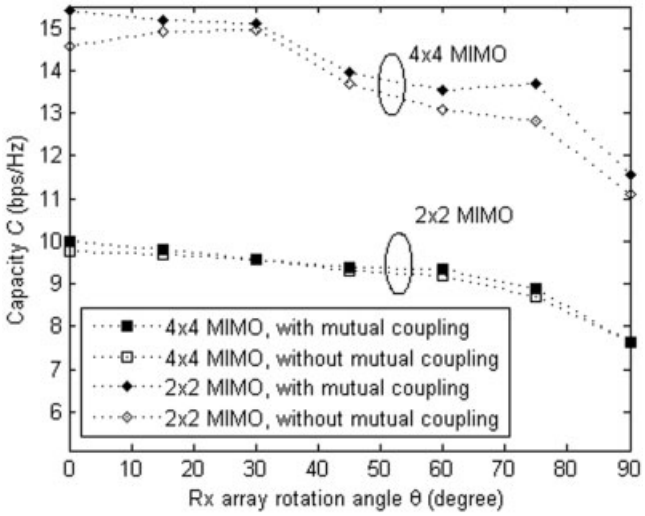

Figure 4 Capacity $C_{P_R=const}$ (bps/Hz) vs. angle of RX array rotation angle θ (in degrees) for $d_T = d_R = 1.0\lambda$, $R = 16\lambda$, $S = 100$, $D = 50\lambda$, and $\rho = 20$ dB

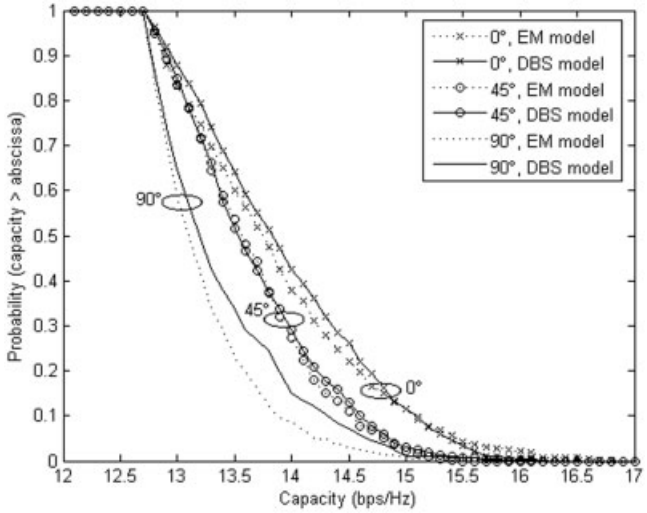

Figure 6 The complementary cumulative distribution function of capacity for the RX array rotation angles of $\theta = 0°$, 45°, and 90° with $N = 2$, $d_T = 1.0\lambda$, $R = 16\lambda$, $S = 75$, $D = 50\lambda$, and $\rho = 20$ dB

$d_T = 1.0\lambda$, $R = 16\lambda$, $D = 50\lambda$, $\rho = 20$ dB, and $S = 75$ without and with interelement coupling included in the model. For the DBS model, the results without mutual coupling were calculated by neglecting coupling matrices in Eq. (8). In the DBS model, the value of the Rician factor was assumed to be $K = 12.5$ dB. The EM model did not require this assumption. To find the right value of the K factor in the DBS model, the case of the spacing $d_R = 0.4\lambda$ capacity was analyzed using the EM model. This spacing is close to the first cross point between including and neglecting mutual coupling, as seen from both the static and statistical cases in Figures 3 and 5, respectively. In the DBS model, various values of K were attempted until the DBS result for capacity matched the one obtained with the EM model. This occurred for $K = 12.5$ dB. As seen in Figure 5, both the EM and DBS models provide good agreement with each other when mutual coupling is included or neglected in the calculations. One problem with the DBS model is that it requires a priori knowledge of the K-factor value. In a real MIMO system, this information can be obtained from the measurements.

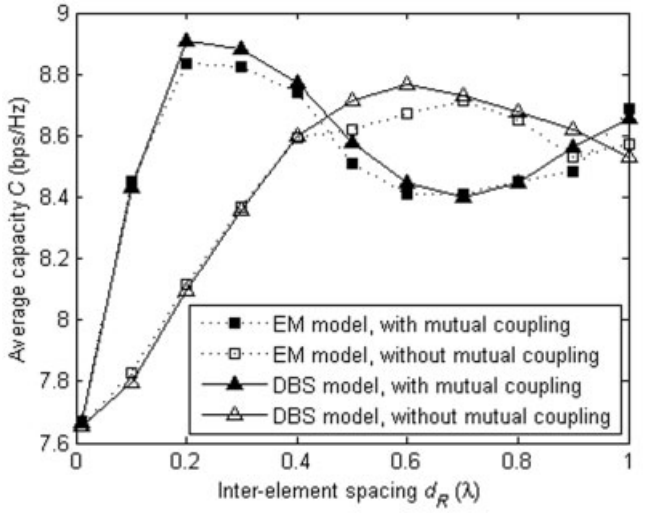

Figure 5 Average capacity $C_{P_R=const}$ (bps/Hz) vs. RX array interelement spacing $d_R(\lambda)$ for $N = 2$, $d_T = 1.0\lambda$, $R = 16\lambda$, $S = 75$, $D = 50\lambda$, and $\rho = 20$ dB

4.2.2. Effect of Array Orientation

Figure 6 shows the complementary cumulative distribution function of capacity for $\theta = 0°$, 45°, and 90° with $N = 2$, $d_T = 1.0\lambda$, $R = 16\lambda$, $S = 75$, $D = 50\lambda$, and $\rho = 20$ dB. In the DBS model, the value of Rician factor was assumed to be $K = 12.5$ dB. The statistical results provide the same trend as that observed in static results, that is, the highest and lowest capacities are produced for the receiving array orientations of $\theta = 0°$ and 90°. The observed trends for distribution functions produced by the EM and DBS models are similar in terms of rotating angle. Small discrepancies between the two indicate that the two models can be interchangeably used to assess the MIMO capacity in the statistical sense.

5. CONCLUSION

In this paper, we have described a simple MIMO system in which TX/RX antennas and scattering objects were formed by wire dipoles. This system has been analyzed in the strict electromagnetic sense with respect to such issues as the impact of array antenna interelement spacing and orientation on capacity. Good agreement among the EM and dual-ring and dual-circle double-bounce scattering models has been obtained, indicating that the latter models can be confidently used while analyzing the performance of MIMO systems operating under mixed LOS/NLOS conditions.

ACKNOWLEDGMENTS

The work presented in this paper has been supported by the Australian Research Council under grant no. DP0450118.

REFERENCES

1. M. Jensen and J.W. Wallace, A review of antennas and propagation for MIMO wireless systems, IEEE Trans Antennas Propagat 52 (2004), 2810–2824.
2. G.J. Foschini and M.J. Gans, On limits of wireless communication in a fading environment when using multiple antennas, Int J Wireless Personal Commun 6 (1998), 311–335.
3. A.J. Paulraj, D.A. Gore, R.U. Nabar, and H. Bolcskei, An overview of

MIMO communications: A key to gigabit wireless, Proc IEEE 92 (2004), 198–218.
4. I.E. Telatar, Capacity of multi-antenna Gaussian channels, Euro Trans Telecommun 10 (1999), 585–595.
5. D. Gesbert, M. Shafi, D. Shiu, P.J. Smith, and A. Najuib, From theory to practice: An overview of MIMO space-time coded wireless systems, IEEE J Sel Areas Commun 21 (2003), 281–302.
6. A.G. Burr, Capacity bounds and estimates for the finite scatterers MIMO wireless channel, IEEE J Sel Areas Commun 21 (2003), 812–818.
7. A. Goldsmith, S.A. Jafar, N. Jindal, and S. Vishwanath, Capacity limits of MIMO channels, IEEE J Sel Areas Commun 21 (2003), 684–702.
8. T. Svantesson and A. Ranheim, Mutual coupling effects on the capacity of multi-element antenna systems, Proc ICASSP Conf 4 (2001), 2485–2488.
9. J.W. Wallace and M.A. Jensen, The capacity of MIMO wireless systems with mutual coupling, VTC Conf, Vancouver, Canada, 2002, pp. 696–700.
10. J. Wallace and M. Jensen, Mutual coupling in MIMO wireless systems: A rigorous network theory analysis, IEEE Trans Wireless Commun 3 (2004), 1317–1325.
11. P.N. Fletcher, M. Dean, and A.R. Nix, Mutual coupling in multi-element array antennas and its influence on MIMO channel capacity, IEEE Electron Lett 39 (2003), 342–344.
12. V. Jungnickel, V. Pohl, and C.V. Helmolt, Capacity of MIMO systems with closely spaced antennas, IEEE Commun Lett 7 (2003), 361–363.
13. M.E. Bialkowski, S. Durrani, K. Bialkowski, and P. Uthansakul, Understanding and analyzing the performance of MIMO systems from the microwave perspective, IEEE Int Microwave Conf, California, 2005, pp. 2251–2254.
14. S. Durrani and M.E. Bialkowski, Effect of mutual coupling on the interference rejection capabilities of linear and circular arrays in CDMA systems, IEEE Trans Antennas Propagat 52 (2004), 1130–1134.
15. C.A. Balanis, Antenna theory: Analysis and design, 2nd ed., Wiley, New York, 1997.
16. B. Clerckx, D.V. Janvier, C. Oestges, and L. Vandendorpe, Mutual coupling effects on the channel capacity and the space–time processing of MIMO communication systems, Proc ICC Conf 4 (2003), 2638–2642.
17. T. Svantesson, Modeling and estimation of mutual coupling in a uniform linear array of dipoles, ICASSP Conf, 1999, pp. 2961–2964.
18. P. Uthansakul, M.E. Bialkowski, S. Durrani, K. Bialkowski, and A. Postula, Effect of line of sight propagation on capacity of an indoor MIMO system, IEEE Int Antennas Propagat Symp, Washington, DC, 2005, pp. 707–710.
19. P. Uthansakul and M.E. Bialkowski, Investigations into MIMO capacity in a mixed LOS/NLOS environment, Asia-Pacific Microwave Conf, Suzhou, China, 2005, pp. 2778–2781.

THREE-ANTENNA MIMO SYSTEM FOR WLAN OPERATION IN A PDA PHONE

Kin-Lu Wong,[1] Chih-Hua Chang,[1] Brian Chen,[2] and Sam Yang[2]
[1] Department of Electrical Engineering
National Sun Yat-Sen University
Kaohsiung 804, Taiwan
[2] Research & Development Division V
Compal Communications, Inc.
Taipei 105, Taiwan

Received 13 December 2005

ABSTRACT: *A multiple input multiple output (MIMO) system using three EMC (electromagnetic compatible) chip antennas in a personal digital assistant (PDA) phone is demonstrated. The three EMC chip antennas are mounted at three corners of the system ground plane of the PDA phone and all generate a wide bandwidth covering the wireless local area network (WLAN) operation in the 2.4-GHz band (2400–2484 MHz). By adding a T-shaped shorted strip in the proposed MIMO antenna system, large improvements in the isolation (S_{12}, S_{13}, and S_{23} all less than −20 dB) between any two antennas of the MIMO system are achieved. Detailed effects of the T-shaped shorted strip on the isolation improvement in the proposed MIMO antenna system are analyzed. Radiation characteristics of the three antennas are also studied.* © 2006 Wiley Periodicals, Inc. Microwave Opt Technol Lett 48: 1238–1242, 2006; Published online in Wiley InterScience (www.interscience.wiley.com). DOI 10.1002/mop.21665

Key words: *antennas; MIMO antennas; WLAN antennas; EMC chip antennas*

1. INTRODUCTION

By using a MIMO system with multiple antennas, a much higher channel capacity over that of the traditional wireless system with a single antenna can be obtained [1]. However, for multiple antennas in mobile devices such as a PDA phone or a smart phone for MIMO operation, good isolation between any two antennas of the MIMO system embedded in the mobile device may not be achieved. This is mainly because the available spaces inside the mobile device for employing the antennas are usually very limited, and this behavior may lead to unacceptable MIMO operation for practical applications.

To overcome the problem, in this paper we propose a promising three-antenna MIMO system embedded in a PDA phone for WLAN operation in the 2.4-GHz band (2400–2484 MHz) [2]. In this study, the EMC chip antennas [3–5] used in the proposed MIMO system are arranged to be at the corners of the system ground plane of the mobile device. In this case, since nearby electronic components inside the mobile device can be placed in close proximity to or in direct contact with the employed antennas, a more compact integration of the associated components inside the mobile device can be obtained. As for achieving improved isolation between any two antennas of the proposed MIMO system, a T-shaped shorted strip is introduced in the proposed design. Detailed experimental and simulation results of the proposed three-antenna MIMO system are presented and analyzed.

2. PROPOSED THREE-ANTENNA MIMO SYSTEM

Figure 1(a) shows the configuration of the proposed three-antenna MIMO system with a T-shaped shorted strip for WLAN operation in a PDA phone. The three antennas used in the study are of the same dimensions, and the detailed dimensions of the metal pattern of the antenna unfolded into a planar structure are shown in Figure 1(b). Note that the three antennas are EMC chip antennas [3–5] with a foam base of $18 \times 10 \times 4$ mm^3, and the antennas are implemented by bending the planar metal plate shown in Figure 1(b), which is obtained by line-cutting a single metal plate (a 0.2-mm-thick copper plate was used in the study), and then mounting it onto the foam base of the antenna. The EMC chip antennas are mainly comprised of a shorted spiral radiating strip, two side ground walls of size 18×4 mm^2 and 10×4 mm^2, and an antenna ground portion of size 18×10 mm^2. Note that the shorted spiral radiating strip has a mean length of about 32 mm, corresponding to about a quarter-wavelength of the frequency at 2442 MHz. In this case, the EMC chip antenna can generate a wide resonant mode covering the 2.4-GHz band for WLAN operation (2400–24834 MHz). For testing the antennas in this study, the 50Ω mini coaxial line is used. The central feeding pin and grounding sheath of the mini coaxial line are connected to the feeding point (point A